Multi-objective Improved Bat Algorithm for Optimizing Fuel Cost, Emission and Active Power Loss in Power System

Gonggui Chen, *Member, IAENG*, Jie Qian, Zhizhong Zhang, and Zhi Sun

***Abstract*— In this paper, a new multi-objective improved bat algorithm (MOIBA) is proposed to solve the constrained multi-objective optimal power flow (MOOPF) problem with contradictory objectives. The proposed MOIBA algorithm, introducing nonlinear inertia weight, global optimal guiding mechanism and monotone random filling model based on extreme (MRFE), can improve the shortcomings of basic bat algorithm which is easy to fall into local optimum. A Pareto-dominant method with constraint priority (PMC) is proposed to ensure that state variables can satisfy the inequality constraints of MOOPF problem. To obtain well-distributed Pareto optimal set (POS), an elite non-dominated sorting method with crowding-distance (ESCD) is adopted. In addition, a fuzzy affiliation approach (FAA) is used to select the best compromise (BC) from the obtained POS. The IEEE 30-bus, IEEE 57-bus and IEEE 118-bus systems are employed to evaluate the effectiveness of MOIBA with four objectives, which includes optimizing basic fuel cost and emission concurrently, optimizing basic fuel cost and active power loss concurrently, optimizing fuel cost with value-point loadings and active power loss concurrently, optimizing basic fuel cost, emission and active power loss concurrently. The legion experimental results obtained by MOIBA, which are contrast to MOPSO and MODE algorithms, validate that MOIBA has definite competitive advantages to achieve satisfactory POS. Furthermore, two performance metrics, generational distance (GD) and spacing (SP), are chosen to estimate the distribution and diversity of Pareto solutions obtained by MOIBA.**

***Index Terms*—Multi-objective Improved Bat Algorithm (MOIBA), Multi-objective Optimal Power Flow (MOOPF), Elite non-dominated sorting approach with crowding-distance (ESCD), generational distance (GD), spacing (SP).**

Manuscript received October 15, 2018; revised December 11, 2018. This work was supported by Innovation Team Program of Chongqing Education Committee (CXTDX201601019), Chongqing University Innovation Team under Grant (KJTD201312) and the National Natural Science Foundation of China (Nos. 51207064 and 61463014).

Gonggui Chen is with the Key Laboratory of Network control & Intelligent Instrument, Chongqing University of Posts and Telecommunications, Ministry of Education, Chongqing 400065, China; Key Laboratory of Complex Systems and Bionic Control, Chongqing University of Posts and Telecommunications, Chongqing 400065, China(e-mail:chenggpower@126.com).

Jie Qian is with the Key Laboratory of Complex Systems and Bionic Control, Chongqing University of Posts and Telecommunications, Chongqing 400065, China (e-mail: qianjie@126.com).

Zhizhong Zhang is with the Key Laboratory of Communication Network and Testing Technology, Chongqing University of Posts and Telecommunications, Chongqing 400065, China (corresponding author, Tel: 023-62461681; e-mail: zhangzztx@163.com).

Zhi Sun is with the Guodian Enshi Hydropower Development, Enshi 445000, China (e-mail: sunzhi24@126.com).

I. Introduction

OPTIMAL power flow (OPF), one of the most influential technologies for optimization and planning of power systems, can achieve better operating status by adjusting control variables which satisfy the secure operation and physical constraints [1-3]. It should be noted that the OPF, which includes both continuous and discrete variables, is a highly-constrained and nonlinear problem [4-6].

Due to severe environment and sharply increasing electricity requirements, the optimization and planning of power systems have received extensive attention [7, 8]. In previous studies, OPF problems were primarily to minimize fuel cost, emission or active power loss separately [9]. In order to measure the operation status of power systems comprehensively, the research hotspot tends to take multiple objective functions into consideration at the same time. The constrained problem with multiple irreconcilable objectives in power systems is called multi-objective optimal power flow (MOOPF) problem.

Solving MOOPF problem is to optimize given objectives simultaneously by adjusting control variables under the premise of satisfying various constraints [10]. Different from seeking the only optimum decision in single-objective optimization, MOOPF aims to obtain a set of optimal solutions and achieve the best compromise (BC) eventually.

In the past years, classic approaches convert multiple objective optimization problems to single-objective ones based on the priority between the decision-maker and solution [11]. However, there are some inevitable drawbacks that traditional methods are not applicable to the situation with unknown tendency of decision-maker and it is almost impossible to find the Pareto optimal solution set (POS) for high-dimensional problems like MOOPF. In addition, to obtain a set of Pareto optimal solutions, a large amount of computational time is required in classic approaches. Therefore, it is imperative to find other advisable methods to handle MOOPF problem.

A great number of evolutionary algorithms are put forward to various optimization problems [12, 13]. Methods such as Multi-Objective Harmony Search algorithm (MOHS) [14], Shuffle Frog Leaping Algorithm(SFLA) [15], a new hybrid optimization algorithm using Modified PSO (MPSO) and SFLA methods (MPSO-SFLA) [16], Fitness Aggregated Genetic Algorithm (FAGA) [17], Flower Pollination Algorithm (FPA) [18] and Multi-Objective Evolutionary

(Advance online publication: 1 February 2019)

Algorithm based Decomposition (MOEA/D) [19] have been effectively applied to solve MOOPF problems.

In this paper, a multi-objective improved bat algorithm (MOIBA) with non-liner weight coefficient and monotone random filling model (MRFE), enhanced by global optimal guidance mechanism, is proposed to tackle MOOPF problem. To evaluate the practicability of MOIBA, different testing cases, which includes optimizing basic fuel cost and emission concurrently, optimizing fuel cost (with value-point loadings) and active power loss concurrently, optimizing basic fuel cost, emission and power loss concurrently, are implemented on IEEE 30-bus, IEEE 57-bus and IEEE 118-bus systems.

The rest of this article is organized as follows: the mathematical model of MOOPF problem is illustrated in Section II. Section III generalizes multi-objective strategies which are necessary to seek POS and BC. Standard bat algorithm and the proposed novel MOIBA approach are presented in Section IV. Section V introduces the application and result analysis of MOIBA on MOOPF problems. Two metrics, generational distance (GD) and spacing (SP), are used to measure the performance of POS in Section VI. Eventually, Section VII gives the conclusions.

II. Mathematical Model

Two main components of MOOPF mathematical model [20, 21], objective functions and constraints, are expressed as follows.

$$\text{minimize } F=(f_1(x,u),\cdots,f_i(x,u),\cdots,f_M(x,u)) \quad (1)$$

$$h_k(x,u)=0,\quad k=1,2,\cdots,H \quad (2)$$

$$g_j(x,u)\le 0,\quad j=1,2,\cdots,G \quad (3)$$

where $f_i(x,u)$ indicates the ith objective function while M ($M \geqslant 2$) represents the number of objectives to be optimized simultaneously. H and G, respectively, indicate the number of equality constraints (ECs) and inequality constraints (ICs). x represents the vector of state variables involving generator active power at slack bus P_{G1}, load bus voltage V_L, generator reactive power Q_G and apparent power of transmission line S. u is the vector of control variables consisting of generator active power outputs at PV buses P_G, generator bus voltages V_G, tap ratios of transformer T and reactive power injection Q_C. x and u, respectively, can be described in (4) and (5).

$$x^T=\left[P_{G1},\mathrm{V}_{L1},\cdots,\mathrm{V}_{LN_{PQ}},\mathrm{Q}_{G1},\cdots,\mathrm{Q}_{GN_G},\mathrm{S}_1,\cdots,S_{N_L}\right] \quad (4)$$

$$u^T=\left[P_{G2},\cdots,P_{GN_G},V_{G1},\cdots,V_{GN_G},T_1,\cdots,T_{N_T},Q_{C1},\cdots,Q_{CN_C}\right] \quad (5)$$

where N_{PQ}, N_G , N_L ,N_T and N_C depict the number of PQ buses, generators ,transmission lines, transformers, and shunt compensators.

A. Objective Functions

There are four objective functions involved in this paper as basic fuel cost, fuel cost with value-point loading, emission and active power loss.

1) Minimization of Basic Fuel Cost

$$Obj1: F_{\text{cost}}=\sum_{i=1}^{N_G}(a_i+b_iP_{Gi}+c_iP_{Gi}^2)\ \$/\mathrm{h} \quad (6)$$

where F_{cost} represents basic fuel cost in units of \$/h. a_i, b_i and c_i are the cost coefficients of the ith generator.

2) Minimization of Emission

$$Obj2: F_{emission}=\sum_{i=1}^{N_G}[\alpha_iP_{Gi}^2+\beta_iP_{Gi}+\gamma_i+\eta_i\exp(\lambda_iP_{Gi})]\ \text{ton/h} \quad (7)$$

where $F_{emission}$ depicts the total emissions such as SO_X and NO_X in units of ton/h while α_i, β_i, γ_i, η_i and λ_i are the emission coefficients of the ith generator.

3) Minimization of Active Power Loss

$$Obj3: F_{Ploss}=\sum_{k=1}^{N_L}g_k[V_i^2+V_j^2-2V_iV_j\cos(\delta_i-\delta_j)]\ \text{MW} \quad (8)$$

where F_{Ploss} is the active power losses in units of MW. V_i, V_j and δ_i, δ_j are the voltage magnitude and voltage angle at bus i and j while g_k represents the conductance of branch k that links bus i to bus j.

4) Minimization of Fuel Cost with Value-point Loadings

$$\begin{aligned}Obj4: F_{\text{cost\_vp}}=\sum_{i=1}^{N_G}(&a_i+b_iP_{Gi}+c_iP_{Gi}^2+\\&\left|d_i\times\sin(e_i\times(P_{Gi}^{\min}-P_{Gi}))\right|)\ \$/\mathrm{h}\end{aligned} \quad (9)$$

where F_{cost_vp} indicates the fuel cost with value-point loadings in the unit of \$/h; d_i ,e_i and $P_{Gi}^{\min}$ are cost coefficients and lower active power at the ith generator bus with value-point loadings.

B. System Constraints

On the premise that all ECs and ICs can be satisfied, the four objectives are optimized.

1) ECs

The ECs reveal typical load flow equations which can be described as (10) and (11).

$$P_{Gi}-P_{Di}-V_i\sum_{j\in N_i}V_j(G_{ij}\cos(\delta_i-\delta_j)+B_{ij}\sin(\delta_i-\delta_j))=0, i\in N \quad (10)$$

$$Q_{Gi}-Q_{Di}-V_i\sum_{j\in N_i}V_j(G_{ij}\sin(\delta_i-\delta_j)-B_{ij}\cos(\delta_i-\delta_j))=0, \mathrm{i}\in \mathrm{N}_{\mathrm{PQ}} \quad (11)$$

where P_{Gi} and Q_{Gi} denote the injected active and reactive power at generator bus i while P_{Di} and Q_{Di} stand for the active and reactive load demand at load bus i. G_{ij} and B_{ij} denote the conductance and susceptance between bus i and j, respectively. N_i represents the amount of nodes linked to bus i (including node i) and N is the number of system buses except slack bus.

2) ICs

Used to limit the bounds of system variables, ICs involve constraints of state variables and control ones.

(1) ICs of control variables

(i) restrictions on generator active power

$$\begin{matrix}P_{Gi}^{\max}-P_{Gi}\ge 0\\P_{Gi}-P_{Gi}^{\min}\ge 0\end{matrix},\ i\in N_G (i\neq 1) \quad (12)$$

(ii) restrictions on voltages at generation buses

$$\begin{matrix}V_{Gi}^{\max}-V_{Gi}\ge 0\\V_{Gi}-V_{Gi}^{\min}\ge 0\end{matrix},\ i\in N_G \quad (13)$$

(iii) restrictions on transformer tap-settings

$$\begin{matrix}T_i^{\max}-T_i\ge 0\\T_i-T_i^{\min}\ge 0\end{matrix},\ i\in N_T \quad (14)$$

(iv) restrictions on reactive power injection

$$\begin{matrix}Q_{Ci}^{\max}-Q_{Ci}\ge 0\\Q_{Ci}-Q_{Ci}^{\min}\ge 0\end{matrix},\ i\in N_C \quad (15)$$

(2) ICs of state variables

(i) restrictions on generator active power at slack bus

$$\begin{aligned} P_{G1}^{\max} - P_{G1} \geq 0 \\ P_{G1} - P_{G1}^{\min} \geq 0 \end{aligned} \quad (16)$$

(ii) restrictions on voltages at load buses

$$\begin{aligned} V_{Li}^{\max} - V_{Li} \geq 0 \\ V_{Li} - V_{Li}^{\min} \geq 0 \end{aligned}, \ i \in N_{PQ} \quad (17)$$

(iii) restrictions on generator reactive power

$$\begin{aligned} Q_{Gi}^{\max} - Q_{Gi} \geq 0 \\ Q_{Gi} - Q_{Gi}^{\min} \geq 0 \end{aligned}, \ i \in N_G \quad (18)$$

(iv) restrictions on apparent power

$$S_{ij}^{\max} - S_{ij} \geq 0, \ ij \in N_L \quad (19)$$

III. Multi-objective Solution Strategy

To achieve POS with fine-quality and select satisfactory BC, three multi-objective strategies are taken into adoption.

A. Pareto-dominant Method with Constraint Priority

The ECs can be satisfied in the process of calculating Newton-Raphson power flow. The ICs are consisted by control variables and state ones. For the former, the control variables of the *i*th individual beyond effective boundary can be adjusted according to principle (20).

$$u_i = \begin{cases} u_i^{\max} & if \ u_i > u_i^{\max} \\ u_i^{\min} & if \ u_i < u_i^{\min} \end{cases} \quad (20)$$

The method to deal with state variables in violation of ICs is completely different from that of control ones. A Pareto-dominant method with constraint priority (PMC) is proposed to handle unqualified state variables and the core concept can be summarized as follows.

(i) Calculate the violation of ICs for *i*th individual $viol(u_i)$ based on (21).

$$viol(u_i) = \sum_{j \in c} \max(g_j(x, u_i), 0) \quad (21)$$

where *c* indicates the number of ICs on state variables.

(ii) Compare the violations of two different sets of control variables u_1 and u_2, which are selected randomly.

(iii) If any of the condition (22) or (23) is satisfied, a conclusion can be drawn that u_1 is more dominant than u_2. It means that u_1 is a Pareto non-dominated solution.

$$viol(u_1) < viol(u_2) \quad (22)$$

$$viol(u_1) = viol(u_2) \cap \begin{cases} f_i(x, u_1) \leq f_i(x, u_2), \forall i \in \{1, 2, ..., M\} \\ f_j(x, u_1) < f_j(x, u_2), \exists j \in \{1, 2, ..., M\} \end{cases} \quad (23)$$

where $f_i(x,u_j)$ represents the *i*th objective function value of the *j*th control variable set.

B. Elite Non-dominated Sorting Method with Crowding Distance

To obtain an evenly-distributed Pareto Frontier (PF), an elite non-dominated sorting method with crowding-distance (ESCD) is employed in this paper [22-24]. Two attributes of each individual, *Rank* and Crowding-distance (*dis*), are determined by the proposed Pareto dominant rule.

1) Rank index

A hybrid population (*HP*) is generated by integrating the parent original population (*POP*) and external archive population (*EAP*). The sizes of *POP* and *EAP* are both chosen as N_a. The rules to define the *Rank* of individuals in *HP* are described as below.

(i) Based on the proposed PMC strategy, all Pareto optimal solutions in *HP* are found and marked as *Rank*=1.

(ii) Eliminate individuals with *Rank*=1 in *HP*. Another set of Pareto non-dominated solutions can be found according to the same dominant strategy and marked as *Rank*=2.

(iii) Repeat the procedures above until every individual in *HP* has a corresponding *Rank* index.

2) dis index

Crowding-distance is used to estimate the degree of intensity between each individual and other two adjacent individuals. Generally, a smaller value of *dis* means a denser solution distribution and a worse population diversity.

Calculate crowding-distance of the *i*th individual according to (24).

$$dis(i) = \sum_{j=1}^{N} \frac{f_j(i-1) - f_j(i+1)}{f_j^{\max} - f_j^{\min}} \quad (24)$$

where $f_j(i\text{-}1)$ is the value of the *j*th optimization goal on the (*i-1*)th individual. f_j^{max} and f_j^{min} ,respectively, indicate maximum and minimum values of the *j*th goal.

Based on indicators of *Rank* and *dis*, all individuals in *HP* are sorted. A smaller label means a better property. A judgment can be made that the *i*th individual is more superior to the *j*th one when either of condition (25) or (26) is satisfied.

$$Rank(i) < Rank(j) \quad (25)$$

$$Rank(i) = Rank(j) \cap dis(i) > dis(j) \quad (26)$$

The former N_a individuals from sorted *HP* are chosen to form new *EAP*. The ESCD strategy avoids difficulty of determining appropriate penalty coefficients in classic methods when dealing with multi-objective problems.

C. Fuzzy Affiliation Approach

A set of optimal solutions, which enables multiple goals to achieve better status synchronously, can be found by taking advantage of the proposed ESCD strategy. The technique of picking out BC from POS, a popular topic of today's research, has great practical significance. The fuzzy affiliation approach (FAA) adopted in this paper is a reasonable way to designate BC and has enormous advantages under the condition that inclination of decision-makers is ambiguous [25].

The satisfaction of the *i*th objective function for the *k*th individual ($s_i(k)$) and total satisfaction value of *k*th Pareto solution ($ts(k)$) are defined as (27) and (28), respectively.

$$s_i(k) = \begin{cases} 1 & f_i \leq f_i^{\min} \\ \dfrac{f_i^{\max} - f_i}{f_i^{\max} - f_i^{\min}} & f_i^{\min} < f_i < f_i^{\max} \\ 0 & f_i \geq f_i^{\max} \end{cases} \quad (27)$$

$$k = 1, 2, \ldots N_a \quad i = 1, 2, \ldots, M$$

$$ts(k) = \frac{\sum_{i=1}^{M} s_i(k)}{\sum_{k=1}^{Na} \sum_{i=1}^{M} s_i(k)} \quad (28)$$

The *ts* index of every Pareto solution is calculated to determine the special solution which is provided with the highest satisfaction, that is, the achieved BC based on FAA.

IV. MULTI-OBJECTIVE IMPROVED BAT ALGORITHM

A. Standard Bat Algorithm

The standard bat algorithm (BA) is inspired by a biological model named echolocation mechanism, which is used for natural bats to forage by ultrasonic wave [26].

The frequency $F(i)$, speed V_i and position X_i of the ith bat are defined as (29), (30) and (31) ,respectively [27, 28]. The local exploration of bat population relies mainly on pulse rate R and loudness A, which are related to the actual distance between bat and prey.

$$F(i) = F_{\min} + r_1 * (F_{\max} - F_{\min}) \tag{29}$$

$$V_i(t) = V_i(t-1) + F(i) * (X_i(t-1) - X_*) \tag{30}$$

$$X_i(t) = X_i(t-1) + V_i(t) \tag{31}$$

where F_{min} and F_{max}, respectively, indicate the minimum and maximum of frequencies. X_* represents the most recent optimum solution while r_1 is a random number between 0 and 1.

The update of BA algorithm is actualized by adjusting F to make bats keep close to the global optimal one continuously. The updated principles of A and R are described as (32) and (33).

$$A_i(t+1) = \tau A_i(t) \tag{32}$$

$$R_i(t+1) = R_0(1-\exp(-lt)) \tag{33}$$

where R_0 is the initial pulse rate. $l(l>0)$ represents the increase coefficient of pulse rate while τ denotes the loudness attenuation coefficient. A is decreasing and R will go to an opposite direction when a better global optimal solution around X_* is determined.

In the single-objective optimization problem, the value of a given objective function is regarded as core indicator to determine the best solution. Undoubtedly, the idea of single-objective is not suitable for strict-constrained problems with multiple contradictory objectives such as MOOPF. In multi-objective optimization studies, the concept of Pareto non-dominated solutions is widely used.

In this paper, the proposed MOIBA enhances speed update manner of BA algorithm and integrates MRFE model innovatively. MOOPF problems considering fuel cost (with value-point loading), emission and active power loss are employed to verify the superiority of MOIBA algorithm as examples.

B. MOIBA Algorithm

BA algorithm has advantages of less parameters and fast convergence, which enables it to be applied to image threshold segmentation and Robust tracking system design successfully [29, 30]. Notwithstanding, the deficiency in weak convergence and difficulty of escaping from local extreme cannot be ignored.

The main improvements of the proposed MOIBA algorithm are summarized as follows.

1) Improved Updated Principle of V

The nonlinear inertia weight coefficient and global optimal guidance mechanism are introduced to improve the speed model of basic BA algorithm. The enhanced manners of speed V and weight coefficient ω are defined as (34) and (35).

$$V_i(t) = \omega(t)V_i(t-1) + r_2F(i)(X_{\mathrm{p}} - X_i(t)) + r_3F(i)(X_{\mathrm{g}} - X_i(t)) \tag{34}$$

$$\omega(t+1) = \omega_{\max} - r_4(\omega_{\max} - \omega_{\min}) + r_5(\omega(t) - (\omega_{\max} + \omega_{\min})/2) \tag{35}$$

where $r_2 \sim r_5$ are random numbers between 0 and 1. X_p and X_g, respectively, indicate local and global optimal solutions as yet. ω_{max} and ω_{min} correspond to the maximum and minimum values of weight coefficient.

2) Improved Updated Principles of R and A

MRFE model is proposed to improve updated principles of R and A. The new manner of pulse rate and loudness can be expressed as (36) and (37).

$$R_i = (R_{start} - R_{end}) * (ite - ite_{\max}) / (1 - ite_{\max}) + R_{end} \tag{36}$$

$$A_i = (A_{end} - A_{start}) * (ite - ite_{\max}) / (1 - ite_{\max}) + A_{start} \tag{37}$$

where ite and ite_{max} ,respectively, indicate the current and maximum iteration of MOIBA. The roles of R_{start} and R_{end} are to limit range of pulse rate while A_{start} and A_{end} specify the range of loudness.

From the point of mathematical theory, the suggested MRFE can meet basic principle of standard BA algorithm, which requires increasing pulse and decreasing loudness when a better solution can be found in local exploration.

The pseudo code of MOIBA is summarized in TABLE I.

TABLE I
PSEUDO CODE OF MOIBA

input: objective function: $f(x)$,x=$[x_1,x_2,\ldots,x_d]^{\mathrm{T}}$
initial parameters of MOIBA: the size of bat population N_a, maximum iteration ite_{max}, the range of frequency $[F_{min}, F_{max}]$, loudness $[A_{start}, A_{end}]$ and pulse rate $[R_{start}, R_{end}]$
Begin
ite=1
while $ite < ite_{max}$
Update speed and position of bat population based on (34) and (31);
Evaluate fitness $f(x)$ of each individual and determine current optimal one named as x_{best};
for ith individual (i=1,2,…,N_a)
Generate a random number between 0 and 1 named *rand1*.
if $rand1>R_i$
Generate x_{per} around x_{best} by a random perturbation;
Generate other random number between 0 and 1 named *rand2* and evaluate $f(x_{per})$;
if ($rand2<A_i$) && (x_{per} dominants x_{best})
The new solution x_{per} is accepted as optimal solution;
Updated R_i and A_i based on (36) and (37);
end if
end if
end for
Renovate the global optimal information;
ite=ite+1;
end while
End
output: x_{best} and $f(x_{best})$

3) Competitive Advantages of MOIBA

The proposed MOIBA approach improves insufficient of basic BA with weak capability of global search and provides a novel avenue for solving MOOPF problem. The competitive advantages of MOIBA lie in the following three aspects.

(i) Compared with linear adjustment of weight coefficient, the above non-linear strategy, which improves solution diversity, can strength local exploitation of standard bat algorithm.

(ii) A guiding mechanism based on global optimal is integrated to improve searching efficiency of basic algorithm. In brief, the proposed global optimal mechanism has good guiding significance to find a better solution near the current best decision.

(iii) The proposed MRFE limits range of *A* and *R* which can improve efficiency as well. On one hand, the model can increase diversity of population. On the other hand, the appropriate range can accelerate the speed of finding a better program in a smaller area near the current best solution

C. *Application of Proposed MOIBA on MOOPF*

In order to verify the practicability and superiority of proposed improved algorithm, MOIBA is recommended to handle MOOPF problems with different cases, which include optimizing basic fuel cost and emission concurrently, optimizing fuel cost (with value-point loading) and active power loss concurrently, optimizing basic fuel cost, emission and active power loss concurrently. The application of novel MOIBA method on MOOPF problem can be summarized as bellows.

(i) Clear the structure and data of test system. The initial bat population (*IBP*) is generated by (38) within valid range of control variables in power system.

$$u_i = u_i^{\min} + rand\left(u_i^{\max} - u_i^{\min}\right) \quad i \in \left[1, N_a\right] \tag{38}$$

(ii) Through Newton-Raphson power flow calculation, $f_j(x,u_i)$, the *j*th objective function value of the *i*th bat in *IBP* (i=1,2,…,N_a), can be obtained. Designate initial local optimal individual X_p and initial global optimal individual X_g randomly.

(iii) Equations (31) and (34) are used to create *POP*. Then adjust the unqualified individuals to meet system constraints based on (20).

(iv) Calculate Newton-Raphson load flow and clarify the values of given optimization goals $f_i(x,u)$ (i=1,2,⋯M) for each individual in *POP*.

(v) Perform local search in specific situations. Generate two random numbers belonging to (0, 1), known as *Rand1* and *Rand2*. For the *i*th bat in *POP*, if $Rand1>R_i$, a random perturbation is acting on $X_{i,p}$ (the optimal position of *i*th bat as yet) to produce a new solution named as X_{per}. Further on, if ($Rand2<Ai$)&(X_{per} dominants $X_{i,p}$), X_{per} will be accepted as the new optimal position of the *i*th bat.

(vi) Integrate *POP* and *EAP* (Parent bat population is regarded as the initial *EAP*). A new *EAP* with size of N_a is renovated on account of ESCD.

(vii) If current iteration meets maximum iteration preset by MOIBA algorithm (ite=ite_{max}), the next step (viii) is executed. Otherwise, repeat from step (iii) for loop execution until termination condition is satisfied.

(viii) The POS from *EAP* is the output and the BC based on FAA is achieved ultimately.

V. Simulation and Result

For the purpose of evaluating the capability of MOIBA method, the novel MOIBA with MOPSO and MODE as comparison are applied on MOOPF problems. Details of testing cases involved in this article are shown in TABLE II.

The mathematical model of object functions is described in Section II. MATLAB 2014a software is employed and all simulation cases are ran on a PC with Intel(R) Core(TM) i5–7500 CPU @ 3.40 GHz with 8GB RAM.

A. *Test Systems*

The structure of the IEEE 30-bus system with 24-dimensional vector, including 6 generators and 30 buses, is shown in Fig. 1. The transformer taps are bounded in 0.9-1.1 p.u. The voltage limits of generator buses and load buses are both restricted within 0.95-1.1 p.u. Details of IEEE 30-bus system are obtained from [31] and TABLE III represents generator coefficients of fuel cost and emission in IEEE 30-bus system.

The principal character of IEEE 57-bus system, whose detail data can be founded in [25, 32], is represented in Fig. 2. The transformer taps are bounded in 0.9-1.1 p.u as well. The shunt capacitor is restricted between 0 and 0.3 p.u. There is a 33-dimensional vector and the range of voltage magnitude for *PQ* and *PV* bus is limited in 0.9-1.1 p.u. Meanwhile, generator coefficients of fuel cost and emission in IEEE 57-bus system are shown in TABLE IV.

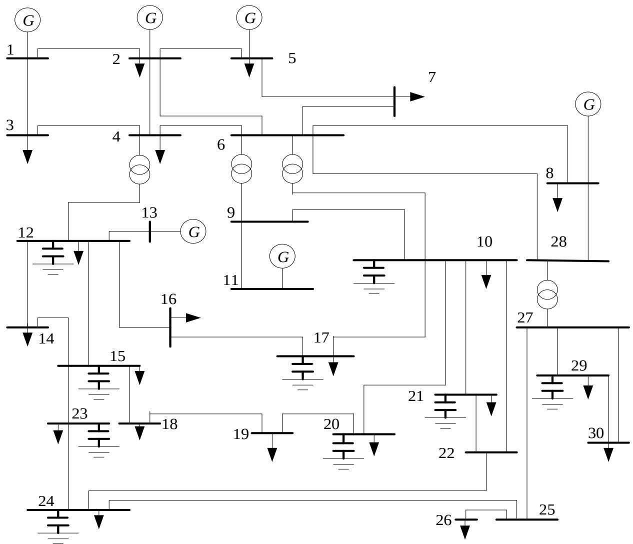

Fig. 1.Single line diagram of IEEE 30-bus system

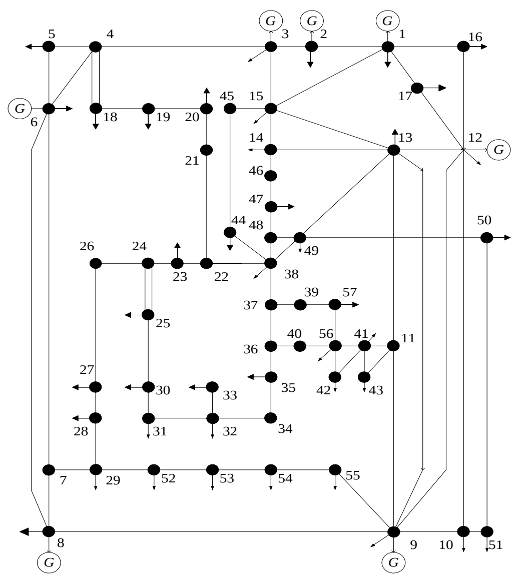

Fig. 2.Single line diagram of IEEE 57-bus system

TABLE II
OBJECT OF CASES

	Obj1	*Obj2*	*Obj3*	*Obj4*	Test system
CASE1	✔	✔			IEEE 30-bus system
CASE2	✔		✔		IEEE 30-bus system
CASE3			✔	✔	IEEE 30-bus system
CASE4	✔	✔	✔		IEEE 30-bus system
CASE5	✔	✔			IEEE 57-bus system
CASE6	✔		✔		IEEE 57-bus system
CASE7	✔	✔			IEEE 118-bus system

TABLE III
FUEL AND EMISSION COEFFICIENTS FOR IEEE 30

	Generating unit					
	G1	G2	G5	G8	G11	G13
Fuel cost						
a	0	0	0	0	0	0
b	2	1.75	1	3.25	3	3
c	0.00375	0.0175	0.0625	0.00834	0.025	0.025
d	18	16	14	12	13	13.5
e	0.037	0.038	0.04	0.045	0.042	0.041
Emission						
α	0.06490	0.05638	0.04586	0.0338	0.04586	0.05151
β	-0.05554	-0.06047	-0.05094	-0.0355	-0.05094	-0.05555
γ	0.04091	0.02543	0.04258	0.05326	0.04258	0.06131
η	0.0002	0.0005	0.000001	0.002	0.000001	0.00001
λ	2.857	3.333	8.000	2.000	8.000	6.667

TABLE IV
FUEL AND EMISSION COEFFICIENTS FOR IEEE 57

	Generating unit						
	G1	G2	G3	G6	G8	G9	G12
Fuel cost							
a	0	0	0	0	0	0	0
b	20	40	20	40	20	40	20
c	0.0775795	0.01	0.25	0.01	0.0222222	0.01	0.0322581
Emission							
α	0.06	0.05	0.04	0.035	0.045	0.05	0.05
β	-0.05	-0.06	-0.05	-0.03	-0.05	-0.04	-0.05
γ	0.04	0.03	0.04	0.035	0.05	0.045	0.06
η	0.00002	0.00005	0.00001	0.00002	0.00004	0.00001	0.00001
λ	0.5	1.5	1	0.5	2	2	1.5

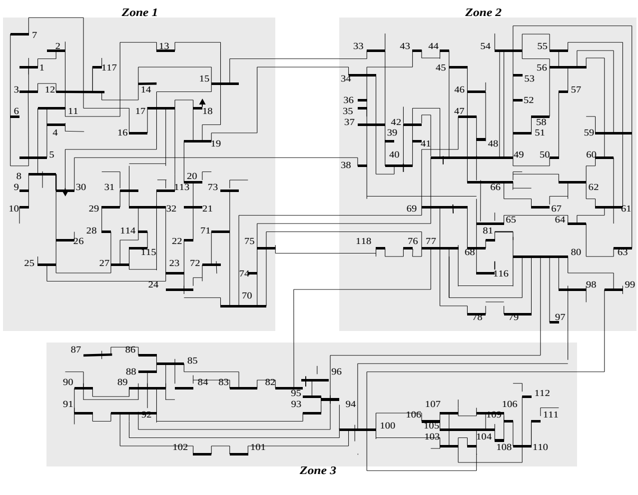

Fig. 3.Single line diagram of IEEE 118-bus system

A larger scale system, IEEE 118-bus system, is employed to evaluate the performance of MOIBA comprehensively. The single line diagram of IEEE 118-bus system with 128-dimensional vector is shown in Fig. 3. The bound of voltage magnitude for *PV* bus are set as 0.9-1.1 p.u. Other detail parameters of IEEE 118-bus system can be obtained in [25].

B. *Algorithm Parameters*

In order to explore the effect of population size and maximum iteration on MOIBA algorithm respectively, the simulation experiments of above two parameters in IEEE 30-bus system are conducted. As an example, basic fuel cost and emission are chosen to optimize concurrently. Fig. 4 represents the PFs obtained by MOIBA in different population sizes with same iteration of 500.

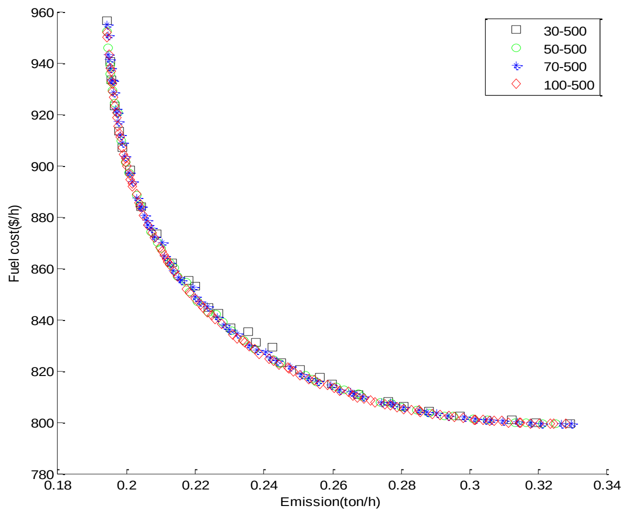

Fig. 4.PFs in different population sizes with iteration of 500

Fig. 4 shows that even 100 individuals, a larger population size, can achieve relative well-distributed PF. It demonstrates the proposed MOIBA algorithm can obtain evenly-distributed PFs with different population sizes. In all experiments performed in this paper, the size of bat population is set as 100.

Then, the performance of MOIBA on different maximum iterations is studied. Fig. 5 shows PFs obtained by MOIBA in different iterations with population size of 100. It can be observed that iteration of 100 obtains the worst PF while iteration of 200 achieves better PF. Fig. 5 also validates that iteration of 300,400 and 500 achieve well-distributed PF with similar efficiency. Therefore, the maximum iteration is chosen as 300 to achieve less computational complexity.

C. Testing on IEEE 30-bus System

1) CASE1: considering basic fuel cost and emission simultaneously

In CASE1, the basic fuel cost and emission as two competing objectives are studied by proposed MOIBA, MOPSO and MODE methods in IEEE 30-bus system. The PFs obtained by above three algorithms are drawn in Fig. 6. It shows that PF achieved by MOIBA is much better than the one obtained by MOPSO. In addition, MOIBA has superior performance than MODE. It is clearly indicated that MOIBA algorithm has great potentiality to achieve well distributed PF. The control variables of MOIBA and other comparison results, sets of 24-dimensional vector, are presented in TABLE V. It can be learned that BC achieved by MOIBA includes 0.2335 ton/h of emission and 831.4750 $/h of fuel cost.

For CASE1, the BCs obtained by different algorithms as comparison are shown in TABLE VI.

2) CASE2: considering basic fuel cost and active power loss simultaneously

In CASE2, basic fuel cost and active power loss are selected as two concurrent optimization objectives. Fig. 7 represents PFs achieved by MOIBA, MOPSO and MODE methods.

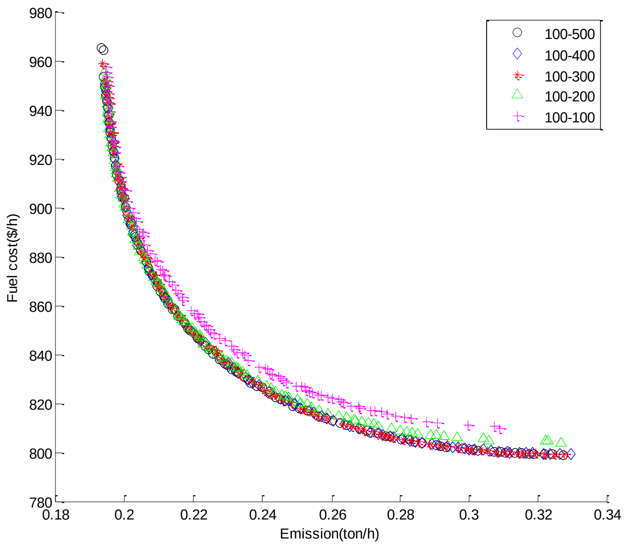

Fig. 5.PFs in different iterations with population size of 100

Fig. 7 shows that MOPSO has the worst PF while MOIBA can obtain a better PF with uniformly distribution. TABLE VII represents control variables of BCs achieved by above three algorithms and two comparison methods. In detail, the BC achieved by MOIBA approach includes 833.6139 $/h of fuel cost and 4.9684 MW of power loss. TABLE VII clearly indicates that MOIBA has certain advantages to obtain better BC when tackling MOOPF problems.

TABLE V
CONTROL BARIABLES OF BC FOR CASE1

control variables	MOPSO	MODE	MOIBA	BSA [33]
P_{G2}(MW)	60.0682	59.7772	57.9465	59.3719
P_{G5}(MW)	27.4352	28.8142	27.7851	27.6576
P_{G8}(MW)	34.9594	35.0000	35.0000	34.9989
P_{G11}(MW)	27.1744	25.6668	26.5897	27.0652
P_{G13}(MW)	24.6857	29.4685	24.8766	26.4502
V_{G1}(p.u.)	1.0997	1.0990	1.0990	1.1000
V_{G2}(p.u.)	1.0896	1.0778	1.0929	1.0855
V_{G5}(p.u.)	1.0617	1.0613	1.0771	1.0606
V_{G8}(p.u.)	1.0580	1.0638	1.0798	1.0757
V_{G11}(p.u.)	1.1000	1.1000	1.1000	1.1000
V_{G13}(p.u.)	1.0590	1.0713	1.0893	1.1000
T_{11}(p.u.)	1.0112	1.0127	0.9979	1.0000
T_{12}(p.u.)	1.0760	1.0413	1.0069	0.9500
T_{15}(p.u.)	0.9778	0.9486	1.0132	1.0000
T_{36}(p.u.)	0.9753	0.9704	1.0182	0.9625
Q_{C10}(p.u.)	0.0381	0.0500	0.0500	3.4844(Mvar)
Q_{C12}(p.u.)	0.0000	0.0500	0.0199	4.5129(Mvar)
Q_{C15}(p.u.)	0.0113	0.0083	0.0000	4.7990(Mvar)
Q_{C17}(p.u.)	0.0278	0.0026	0.0000	4.9965(Mvar)
Q_{C20}(p.u.)	0.0132	0.0072	0.0286	3.9809(Mvar)
Q_{C21}(p.u.)	0.0460	0.0343	0.0474	4.7684(Mvar)
Q_{C23}(p.u.)	0.0500	0.0192	0.0361	3.8535(Mvar)
Q_{C24}(p.u.)	0.0359	0.0500	0.0500	4.2332(Mvar)
Q_{C29}(p.u.)	0.0168	0.0391	0.0500	1.6339(Mvar)
Obj1 ($/h)	833.8682	840.5655	**831.4750**	835.0199
Obj2(ton/h)	0.2448	0.2263	**0.2335**	0.2425

TABLE VI
COMPARISON RESULTS OF BCs FOR CASE1

Comparison	Fuel cost($/h)	Emission(ton/h)
MOIBA	831.4750	0.2335
MOMICA [7]	865.066	0.2221
MSLFA [15]	867.713	0.2247
CIWO [34]	820.2154	0.296
AGSO [35]	843.5473	0.2539
MGBICA [32]	830.8514	0.2484
ESDE-MC [36]	830.7185	0.2483

3) CASE3: considering active power loss and fuel cost with value-point loading simultaneously

In CASE3, the power loss and fuel cost with value-point loading are chosen to optimize simultaneously. The PFs achieved by different methods are shown in Fig. 8. Contrast to MOPSO and MODE, MOIBA method achieves preferable PF. The BC of MOIBA includes 857.3445 $/h of fuel cost with value-point loading and 5.9166 MW of power loss. The control variables of BCs can be found in TABLE VIII.

4) CASE4: considering basic fuel cost, emission and active power loss simultaneously

In CASE4, three objectives covered in this paper including basic fuel cost, emission and active power loss, are optimized concurrently.

Fig. 9 shows the PFs obtained by MOIBA, MOPSO, and MODE algorithms, respectively. The control variables of BC are presented in TABLE IX. It is noteworthy that BCs determined by MOIBA includes 884.3171$/h of fuel cost, 0.2043ton/h of emission and 3.7975MW of active power loss.

TABLE VII
CONTROL BARIABLES OF BC FOR CASE2

control variables	MOPSO	MODE	MOIBA	MSA [31]	MOHS [37]
P_{G2}(MW)	50.5747	58.0214	53.1167	55.0797	51.5253
P_{G5}(MW)	31.0206	32.1441	32.1204	38.2097	27.8550
P_{G8}(MW)	33.4833	35.0000	35.0000	34.9995	34.9822
P_{G11}(MW)	30.0000	25.7647	26.8188	29.9947	28.6026
P_{G13}(MW)	26.4376	23.5184	23.7295	26.8439	27.1048
V_{G1}(p.u.)	1.0988	1.0998	1.1000	1.0694	1.0868
V_{G2}(p.u.)	1.0899	1.0924	1.0936	1.0586	1.0771
V_{G5}(p.u.)	1.0728	1.0723	1.0720	1.0346	1.0535
V_{G8}(p.u.)	1.0813	1.0803	1.0783	1.0429	1.0576
V_{G11}(p.u.)	1.0990	1.0851	1.0999	1.0895	1.0896
V_{G13}(p.u.)	1.0842	1.0965	1.1000	1.0549	1.0845
T_{11}(p.u.)	1.0496	1.0270	1.0328	1.0240	0.9696
T_{12}(p.u.)	0.9235	0.9238	0.9002	0.9628	1.0026
T_{15}(p.u.)	1.0707	1.0039	0.9819	0.9896	0.9893
T_{36}(p.u.)	0.9779	0.9628	0.9658	0.9760	0.9781
Q_{C10}(p.u.)	0.0247	0.0500	0.0165	1.9821(Mvar)	0.0465
Q_{C12}(p.u.)	0.0072	0.0500	0.0477	1.6860(Mvar)	0.0105
Q_{C15}(p.u.)	0.0381	0.0462	0.0492	4.1810(Mvar)	0.0464
Q_{C17}(p.u.)	0.0062	0.0418	0.0465	5.0000(Mvar)	0.0483
Q_{C20}(p.u.)	0.0500	0.0288	0.0500	3.6295(Mvar)	0.0450
Q_{C21}(p.u.)	0.0104	0.0500	0.0494	4.9583(Mvar)	0.0423
Q_{C23}(p.u.)	0.0203	0.0330	0.0143	2.8818(Mvar)	0.0483
Q_{C24}(p.u.)	0.0175	0.0500	0.0458	4.9987(Mvar)	0.0164
Q_{C29}(p.u.)	0.0000	0.0269	0.0281	2.5955(Mvar)	0.0093
Obj1($/h)	837.1553	835.8013	**833.6139**	859.1915	832.6709
Obj3(MW)	5.0932	4.9275	**4.9684**	4.5404	5.3143

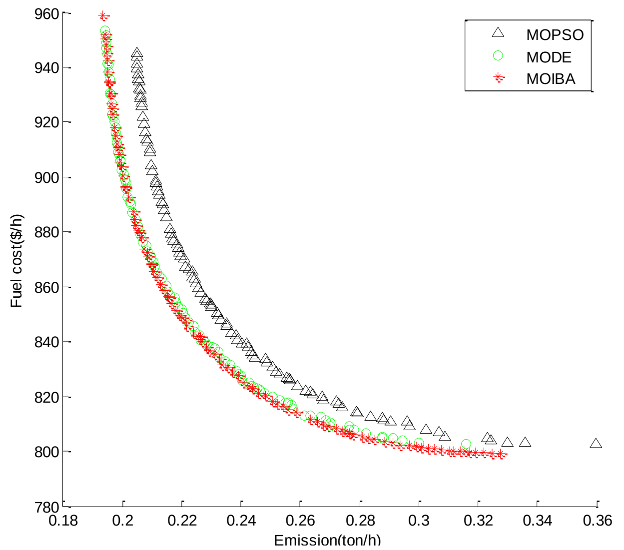

Fig. 6.PFs obtained by different methods for CASE1

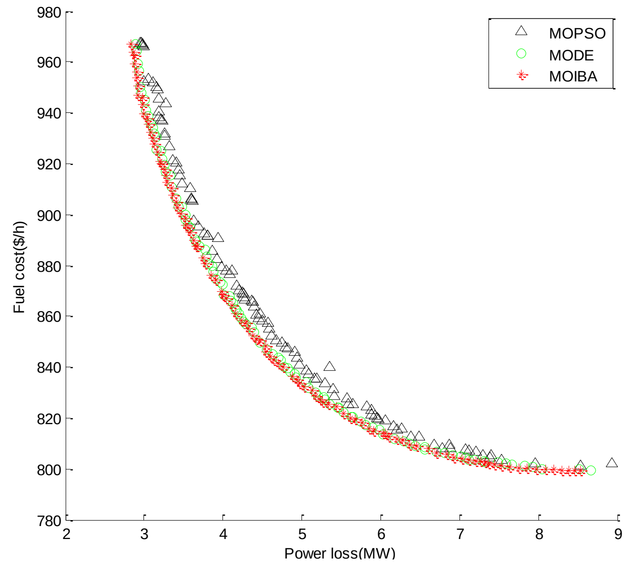

Fig. 7.PFs obtained by different methods for CASE2

TABLE VIII
CONTROL BARIABLES OF BC FOR CASE3

control variables	MOPSO	MODE	MOIBA
P_{G2}(MW)	54.5373	47.2127	51.8665
P_{G5}(MW)	30.2333	31.5679	28.3434
P_{G8}(MW)	33.3049	34.9384	35.0000
P_{G11}(MW)	20.4693	24.1176	22.8740
P_{G13}(MW)	15.4956	14.7819	15.6919
V_{G1}(p.u.)	1.1000	1.1000	1.1000
V_{G2}(p.u.)	1.0882	1.0863	1.0899
V_{G5}(p.u.)	1.0430	1.0648	1.0678
V_{G8}(p.u.)	1.0659	1.0731	1.0840
V_{G11}(p.u.)	1.1000	1.0794	1.1000
V_{G13}(p.u.)	1.0788	1.0961	1.1000
T_{11}(p.u.)	1.0804	1.0664	0.9908
T_{12}(p.u.)	0.9323	0.9000	0.9523
T_{15}(p.u.)	0.9904	0.9980	1.0039
T_{36}(p.u.)	0.9852	0.9792	0.9821
Q_{C10}(p.u.)	0.0000	0.0343	0.0215
Q_{C12}(p.u.)	0.0382	0.0430	0.0457
Q_{C15}(p.u.)	0.0095	0.0364	0.0500
Q_{C17}(p.u.)	0.0200	0.0161	0.0500
Q_{C20}(p.u.)	0.0436	0.0292	0.0410
Q_{C21}(p.u.)	0.0500	0.0500	0.0433
Q_{C23}(p.u.)	0.0476	0.0143	0.0442
Q_{C24}(p.u.)	0.0158	0.0500	0.0500
Q_{C29}(p.u.)	0.0454	0.0095	0.0143
Obj3(MW)	6.1456	5.7820	**5.9166**
Obj4($/h)	858.3259	862.0571	**857.3445**

Additionally, several special solutions in CASE4 which include BC, optimization *A* with minimum fuel cost, optimization *B* with minimum emission and optimization *C* with minimum active power loss, can be observed visually in Fig. 10.

D. Testing on IEEE 57-bus System

1) CASE5: considering basic fuel cost and emission simultaneously

In CASE5, the basic fuel cost and emission as two simultaneous optimization objectives are studied by the proposed MOIBA approach. Fig. 11 shows PFs obtained by three algorithms with 30 independent experiments and it indicates that MOIBA and MODE methods are able to achieve evenly distributed PF while the PF obtained by MOPSO algorithm is more densely distributed. Consequently, MOIBA is provided with obvious superior performance. It can be seen from TABLE X that BC of MOIBA includes 43265.8262$/h of fuel cost and 1.2097 ton/h of emission.

2) CASE6: considering basic fuel cost and active power loss simultaneously

In CASE6, basic fuel cost and active power loss as two competing objectives are studied in IEEE 57-bus system. The obtained PFs are shown in Fig. 12, which states that the PF achieved by MOIBA method is much high-caliber than PFs obtained by MOPSO and MODE.

For CASE6, the control variables of MOIBA and other two algorithms, sets of 33-dimensional vector, are presented in TABLE XI. It is worthy to mention that BC determined by MOIBA includes 42098.7213$/h of fuel cost and 11.4759 MW of power loss.

The results of two testing cases on IEEE 57-bus system testify that MOIBA approach has great competitive advantages for exploring high-performance BCs in power systems with more complex structures.

E. Testing on IEEE 118-bus System

In CASE7, basic fuel cost and emission are chosen to optimize at the same time on IEEE 118-bus system. However, MOPSO can hardly get an evenly-distributed PF in CASE7. The PFs, which are obtained by MODE and MOIBA algorithms respectively, are shown in Fig. 13.

TABLE IX
CONTROL BARIABLES OF BC FOR CASE4

control variables	MOPSO	MODE	MOIBA
P_{G2}(MW)	61.5448	61.5518	65.2252
P_{G5}(MW)	38.6603	42.4018	38.4875
P_{G8}(MW)	35.0000	35.0000	35.0000
P_{G11}(MW)	30.0000	30.0000	30.0000
P_{G13}(MW)	40.0000	27.4023	34.7433
V_{G1}(p.u.)	1.1000	1.0990	1.0992
V_{G2}(p.u.)	1.0935	1.0916	1.0969
V_{G5}(p.u.)	1.0687	1.0525	1.0757
V_{G8}(p.u.)	1.0849	1.0765	1.0873
V_{G11}(p.u.)	1.0864	1.0806	1.0929
V_{G13}(p.u.)	1.0771	1.1000	1.0971
T_{11}(p.u.)	1.1000	1.0041	1.0230
T_{12}(p.u.)	0.9602	0.9657	0.9507
T_{15}(p.u.)	0.9742	0.9988	0.9920
T_{36}(p.u.)	0.9881	0.9766	0.9773
Q_{C10}(p.u.)	0.0364	0.0425	0.0493
Q_{C12}(p.u.)	0.0000	0.0446	0.0500
Q_{C15}(p.u.)	0.0500	0.0091	0.0000
Q_{C17}(p.u.)	0.0500	0.0271	0.0383
Q_{C20}(p.u.)	0.0000	0.0500	0.0466
Q_{C21}(p.u.)	0.0000	0.0250	0.0443
Q_{C23}(p.u.)	0.0462	0.0500	0.0144
Q_{C24}(p.u.)	0.0500	0.0323	0.0434
Q_{C29}(p.u.)	0.0500	0.0500	0.0249
Obj1(MW)	3.8771	3.9783	**3.7975**
Obj2(ton/h)	0.2021	0.2093	**0.2043**
Obj3($/h)	891.9333	879.3475	**884.3171**

Fig. 13 suggests that MODE and MOIBA algorithms can effectively solve MOOPF problem which aims to optimize basic fuel cost and emission concurrently. The control variables of BC, obtained by MOIBA with 2.5255 ton/h of emission and 60337.2739 $/h of fuel cost, are represented on TABLE XII in detail. In contrast to MODE, MOIBA algorithm is much more outstanding for solving MOOPF problem in large scale power systems.

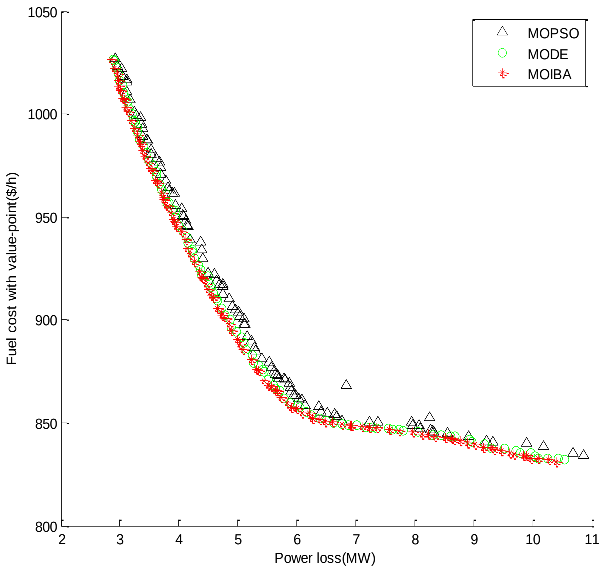

Fig. 8.PFs obtained by different methods for CASE3

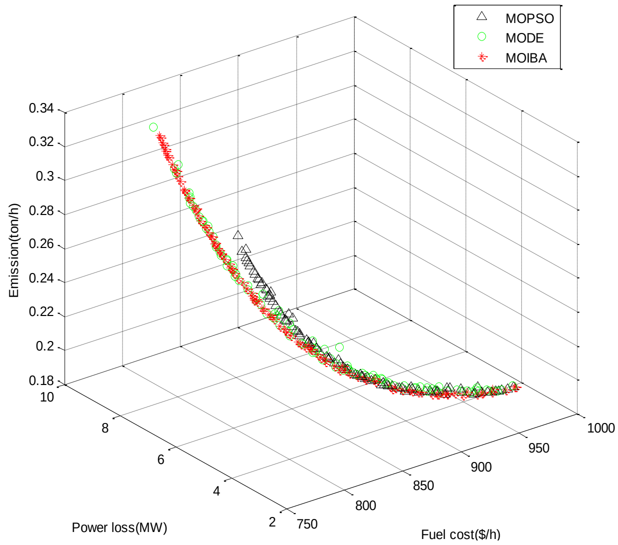

Fig. 9.PFs obtained by different methods for CASE4

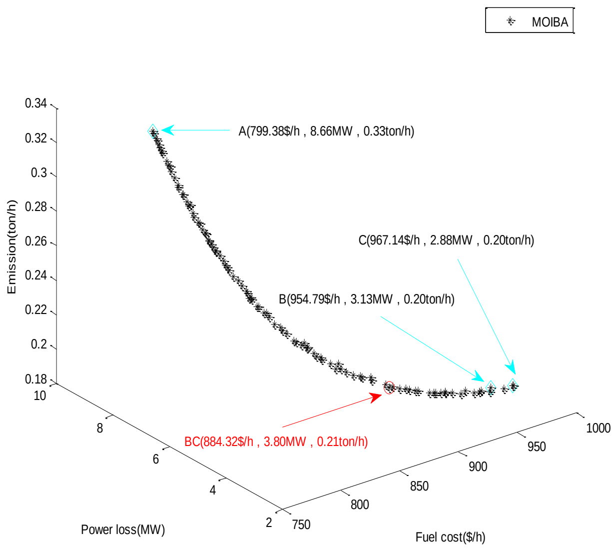

Fig. 10. Special optimization solutions for CASE4

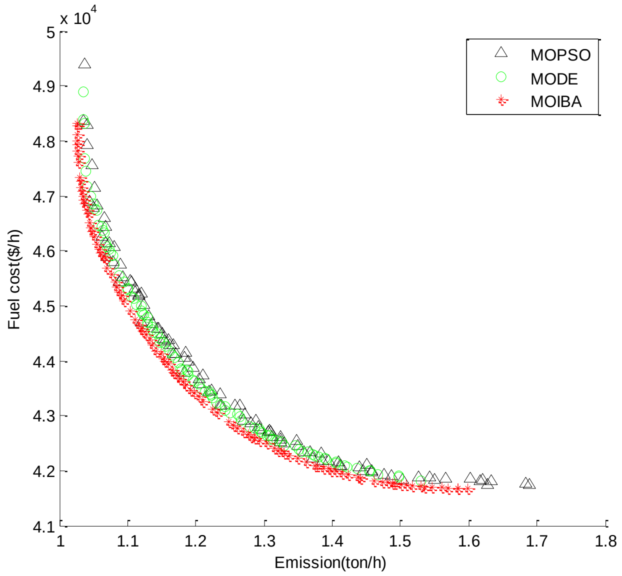

Fig. 11. PFs obtained by different methods for CASE5

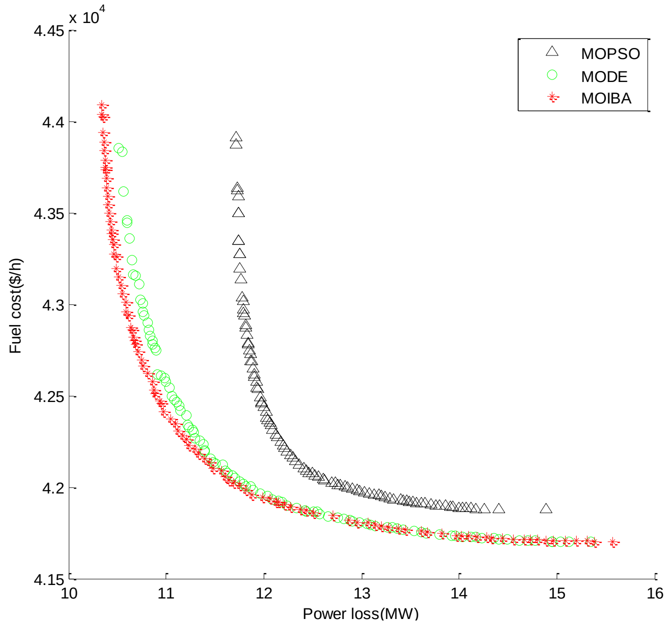

Fig. 12. PFs obtained by different methods for CASE6

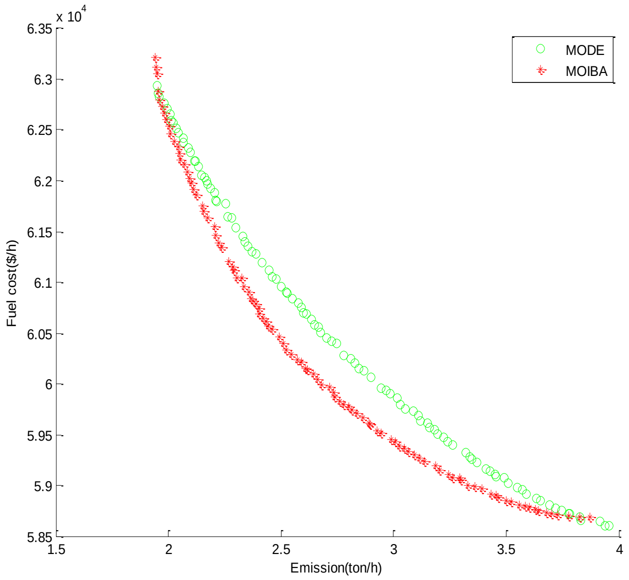

Fig. 13. PFs obtained by different methods for CASE7

TABLE X
CONTROL BARIABLES OF BC FOR CASE5

control variables	MOPSO	MODE	MOIBA
P_{G2}(MW)	98.3137	100.0000	99.9535
P_{G3}(MW)	92.8970	101.7033	95.6767
P_{G6}(MW)	100.0000	100.0000	99.9346
P_{G8}(MW)	332.9963	343.1563	354.0412
P_{G9}(MW)	100.0000	99.4093	99.902.
P_{G12}(MW)	295.6566	290.0402	295.9331
V_{G1}(p.u.)	1.1000	1.0417	1.0992
V_{G2}(p.u.)	1.1000	1.0295	1.0986
V_{G3}(p.u.)	1.1000	1.0103	1.0964
V_{G6}(p.u.)	1.1000	1.0214	1.0995
V_{G8}(p.u.)	1.1000	1.0317	1.0984
V_{G9}(p.u.)	1.1000	1.0173	1.0989
V_{G12}(p.u.)	1.1000	0.9957	1.0857
T_{19}(p.u.)	0.9000	0.9000	1.0795
T_{20}(p.u.)	1.1000	0.9972	1.0208
T_{31}(p.u.)	0.9630	1.0130	0.9811
T_{35}(p.u.)	1.0529	1.0381	0.9934
T_{36}(p.u.)	1.1000	0.9286	1.0251
T_{37}(p.u.)	1.0289	1.0711	0.9811
T_{41}(p.u.)	1.0485	0.9425	1.0247
T_{46}(p.u.)	1.0437	0.9034	0.9997
T_{54}(p.u.)	0.9470	0.9000	1.0721
T_{58}(p.u.)	1.1000	0.9056	1.0060
T_{59}(p.u.)	1.0224	0.9304	1.0093
T_{65}(p.u.)	1.0335	0.9000	1.0346
T_{66}(p.u.)	1.0300	0.9169	0.9815
T_{71}(p.u.)	1.0247	0.9430	0.9703
T_{73}(p.u.)	1.0334	1.1000	0.9502
T_{76}(p.u.)	0.9222	0.9918	1.0048
T_{80}(p.u.)	1.0688	1.0138	1.0201
Q_{C18}(p.u.)	0.0136	0.0077	0.2470
Q_{C25}(p.u.)	0.3000	0.0559	0.1761
Q_{C53}(p.u.)	0.1321	0.1062	0.1185
Obj1 ($/h)	43786.3697	43823.4856	**43265.8262**
Obj2(ton/h)	1.1835	1.1793	**1.2097**

TABLE XI
CONTROL BARIABLES OF BC FOR CASE6

control variables	MOPSO	MODE	MOIBA
P_{G2}(MW)	100.0000	61.1155	53.4086
P_{G3}(MW)	57.9772	65.5631	62.6900
P_{G6}(MW)	100	91.7861	89.8593
P_{G8}(MW)	351.1694	370.9687	377.9932
P_{G9}(MW)	100.0000	99.9879	99.9232
P_{G12}(MW)	410.0000	410.0000	410.0000
V_{G1}(p.u.)	1.1000	1.0113	1.0536
V_{G2}(p.u.)	1.1000	1.0074	1.0467
V_{G3}(p.u.)	1.1000	1.0096	1.0436
V_{G6}(p.u.)	1.1000	1.0232	1.0521
V_{G8}(p.u.)	1.1000	1.0369	1.0613
V_{G9}(p.u.)	1.1000	1.0234	1.0481
V_{G12}(p.u.)	1.1000	1.0068	1.0337
T_{19}(p.u.)	0.9000	0.9793	1.0350
T_{20}(p.u.)	1.1000	0.9884	0.9496
T_{31}(p.u.)	1.1000	1.0271	0.9837
T_{35}(p.u.)	1.1000	1.0469	1.0267
T_{36}(p.u.)	1.1000	1.0825	1.0055
T_{37}(p.u.)	1.1000	1.0033	1.0597
T_{41}(p.u.)	1.0891	0.9520	0.9682
T_{46}(p.u.)	0.9000	0.9744	0.9558
T_{54}(p.u.)	0.9000	0.9178	0.9893
T_{58}(p.u.)	1.1000	0.9214	0.9281
T_{59}(p.u.)	1.0230	0.9256	0.9192
T_{65}(p.u.)	1.1000	0.9453	0.9525
T_{66}(p.u.)	0.9967	0.9000	0.9441
T_{71}(p.u.)	1.1000	0.9003	0.9527
T_{73}(p.u.)	1.1000	1.0401	0.9421
T_{76}(p.u.)	0.9000	0.9606	1.0606
T_{80}(p.u.)	1.1000	0.9491	0.9688
Q_{C18}(p.u.)	0.0000	0.1902	0.2343
Q_{C25}(p.u.)	0.2463	0.1945	0.1310
Q_{C53}(p.u.)	0.1480	0.1408	0.1876
Obj1 ($/h)	42171.7722	42137.9664	**42098.7213**
Obj3 (MW)	12.2707	11.4795	**11.4759**

VI. METRICS

To evaluate the distribution and diversity of POS achieved by the proposed MOIBA method, two performance metrics known as generational distance and spacing are adopted.

A. SP

The SP criteria is adopted to measure variance range of neighbouring vectors in the non-dominated solutions[11] and it can be described as (39).

TABLE XII
CONTROL BARIABLES OF BC FOR CASE7

control variables	MODE	MOIBA	control variables	MODE	MOIBA
P_{G4}(MW)	5.4173	5.1990	V_{G26}(p.u.)	1.0164	0.9843
P_{G6}(MW)	5.1624	7.6612	V_{G27}(p.u.)	1.0354	1.0208
P_{G8}(MW)	22.0625	7.1524	V_{G31}(p.u.)	1.0144	1.0183
P_{G10}(MW)	253.0953	237.2936	V_{G32}(p.u.)	0.9767	1.0418
P_{G12}(MW)	259.1453	190.5417	V_{G34}(p.u.)	0.9752	1.0353
P_{G15}(MW)	23.9557	13.2629	V_{G36}(p.u.)	1.0225	1.0426
P_{G18}(MW)	44.7107	71.0827	V_{G40}(p.u.)	1.0490	1.0250
P_{G19}(MW)	5.2598	5.1740	V_{G42}(p.u.)	0.9992	1.0450
P_{G24}(MW)	5.2994	11.1093	V_{G46}(p.u.)	1.0213	1.0172
P_{G25}(MW)	100.0411	100.0000	V_{G49}(p.u.)	0.9961	1.0057
P_{G26}(MW)	107.7346	100.3920	V_{G54}(p.u.)	0.9998	0.9910
P_{G27}(MW)	21.5025	8.3718	V_{G55}(p.u.)	0.9968	0.9925
P_{G31}(MW)	12.5127	20.2615	V_{G56}(p.u.)	0.9895	0.9919
P_{G32}(MW)	97.5355	41.7051	V_{G59}(p.u.)	1.0411	1.0231
P_{G34}(MW)	8.0087	14.5497	V_{G61}(p.u.)	1.0303	1.0081
P_{G36}(MW)	25.3839	25.0005	V_{G62}(p.u.)	0.9781	1.0215
P_{G40}(MW)	14.6486	8.6687	V_{G65}(p.u.)	1.0181	0.9939
P_{G42}(MW)	8.0678	8.1375	V_{G66}(p.u.)	0.9958	1.0425
P_{G46}(MW)	48.6055	45.1317	V_{G69}(p.u.)	0.9848	1.0188
P_{G49}(MW)	125.1130	224.6722	V_{G70}(p.u.)	1.0360	1.0344
P_{G54}(MW)	214.6151	147.2099	V_{G72}(p.u.)	1.0946	0.9842
P_{G55}(MW)	25.0048	32.3252	V_{G73}(p.u.)	1.0033	0.9940
P_{G56}(MW)	25.0175	39.2805	V_{G74}(p.u.)	0.9925	0.9824
P_{G59}(MW)	58.0430	52.6131	V_{G76}(p.u.)	1.0188	1.0374
P_{G61}(MW)	200.0000	128.5648	V_{G77}(p.u.)	1.0456	1.0309
P_{G62}(MW)	29.1607	81.9615	V_{G80}(p.u.)	1.0143	1.0297
P_{G65}(MW)	220.7434	419.9996	V_{G85}(p.u.)	0.9976	0.9808
P_{G66}(MW)	246.6875	261.9751	V_{G87}(p.u.)	1.0441	0.9897
P_{G69}(MW)	44.6365	30.0000	V_{G89}(p.u.)	1.0527	1.0402
P_{G70}(MW)	20.1894	21.1736	V_{G90}(p.u.)	0.9747	1.0030
P_{G72}(MW)	5.8187	6.1954	V_{G91}(p.u.)	1.0021	1.0180
P_{G73}(MW)	5.0721	8.8132	V_{G92}(p.u.)	1.0891	1.0362
P_{G74}(MW)	25.4764	29.1304	V_{G99}(p.u.)	0.9168	1.0361
P_{G76}(MW)	63.0482	35.1254	V_{G100}(p.u.)	1.0156	1.0450
P_{G77}(MW)	211.2439	214.8409	V_{G103}(p.u.)	1.0127	1.0165
P_{G80}(MW)	26.3544	59.9553	V_{G104}(p.u.)	1.0263	1.0180
P_{G85}(MW)	10.2409	21.9709	V_{G105}(p.u.)	1.0274	1.0121
P_{G87}(MW)	239.0276	165.8360	V_{G107}(p.u.)	1.0222	1.0031
P_{G89}(MW)	133.6475	74.9546	V_{G110}(p.u.)	1.0430	1.0226
P_{G90}(MW)	8.0143	10.4533	V_{G111}(p.u.)	1.0642	1.0221
P_{G91}(MW)	28.6422	30.5562	V_{G112}(p.u.)	1.0513	1.0260
P_{G92}(MW)	149.3441	138.6102	V_{G113}(p.u.)	1.0157	1.0293
P_{G99}(MW)	146.4664	116.6826	V_{G116}(p.u.)	0.9813	1.0656
P_{G100}(MW)	189.8467	192.8604	T_{8}(p.u.)	1.0083	0.9588
P_{G103}(MW)	15.5795	11.2980	T_{32}(p.u.)	1.0505	1.0010
P_{G104}(MW)	31.6193	27.5064	T_{36}(p.u.)	1.0519	0.9944
P_{G105}(MW)	25.0000	36.0719	T_{51}(p.u.)	1.0117	0.9377
P_{G107}(MW)	8.0514	14.2995	T_{93}(p.u.)	1.0112	0.9624
P_{G110}(MW)	25.2384	33.5927	T_{95}(p.u.)	0.9513	1.0147
P_{G111}(MW)	27.9984	37.9701	T_{102}(p.u.)	1.0526	0.9234
P_{G112}(MW)	25.8891	28.4573	T_{107}(p.u.)	0.9497	0.9013
P_{G113}(MW)	58.2361	41.2603	T_{127}(p.u.)	0.9912	1.0287
P_{G116}(MW)	31.6475	37.6642	Q_{C34}(p.u.)	0.0588	0.1364
V_{G1}(p.u.)	1.0155	1.0117	Q_{C44}(p.u.)	0.1448	0.0746
V_{G4}(p.u.)	1.0176	1.0265	Q_{C45}(p.u.)	0.0678	0.1274
V_{G6}(p.u.)	1.0148	1.0048	Q_{C46}(p.u.)	0.2075	0.1277
V_{G8}(p.u.)	1.0674	1.0357	Q_{C48}(p.u.)	0.0684	0.0468
V_{G10}(p.u.)	1.0127	0.9921	Q_{C74}(p.u.)	0.2554	0.2252
V_{G12}(p.u.)	0.9905	0.9864	Q_{C79}(p.u.)	0.2033	0.1970
V_{G15}(p.u.)	0.9759	1.0410	Q_{C82}(p.u.)	0.2526	0.0967
V_{G18}(p.u.)	0.9772	0.9818	Q_{C83}(p.u.)	0.0048	0.1459
V_{G19}(p.u.)	1.0150	1.0528	Q_{C105}(p.u.)	0.1014	0.2628
V_{G24}(p.u.)	1.0091	1.0536	Q_{C107}(p.u.)	0.0037	0.2401
V_{G25}(p.u.)	0.9956	0.9911	Q_{C110}(p.u.)	0.0723	0.0116
			Obj1 ($/h)	60508.7802	**60337.2739**
			Obj2(ton/h)	2.6747	**2.5255**

TABLE XIII
THE MEAN AND STANDARD DEVIATION OF TWO INDEXES FOR CASE1 AND CASE2

criteria	CASE1				CASE2			
	GD		SP		GD		SP	
algorithm	mean	deviation	mean	deviation	mean	deviation	mean	deviation
MOPSO	0.0980	0.0674	0.6037	0.2128	0.0935	0.0222	0.7654	0.2018
MODE	0.0715	0.0139	0.9691	0.0663	0.0715	0.0137	0.8648	0.1087
MOIBA	0.0673	0.0129	0.8523	0.0534	0.0684	0.0131	0.8746	0.0558

TABLE XIV
THE MEAN AND STANDARD DEVIATION OF TWO INDEXES FOR CASE3 AND CASE4

criteria	CASE3				CASE4			
	GD		SP		GD		SP	
algorithm	mean	deviation	mean	deviation	mean	deviation	mean	deviation
MOPSO	0.0961	0.0196	0.8255	0.2389	0.0903	0.0188	0.6876	0.4082
MODE	0.0748	0.0143	1.0204	0.0710	0.0741	0.0143	1.1139	0.1223
MOIBA	0.0764	0.0145	0.9669	0.0566	0.0763	0.0148	1.1166	0.0931

TABLE XV
THE MEAN AND STANDARD DEVIATION OF TWO INDEXES FOR CASE5 AND CASE6

criteria	CASE5				CASE6			
	GD		SP		GD		SP	
algorithm	mean	deviation	mean	deviation	mean	deviation	mean	deviation
MOPSO	0.5241	0.1382	100.9416	47.6487	4.5958	1.6522	6.0090	19.4654
MODE	0.5086	0.1464	59.5999	22.6101	1.3449	0.5191	26.7961	15.6770
MOIBA	0.4320	0.1028	35.1443	3.4877	0.3728	0.1097	18.3403	3.6779

TABLE XVI
THE MEAN AND STANDARD DEVIATION OF TWO INDEXES FOR CASE7

criteria	CASE7			
	GD		SP	
algorithm	mean	deviation	mean	deviation
MODE	1.8789	1.2259	15.8141	6.8879
MOIBA	0.7999	0.3439	18.4330	2.2900

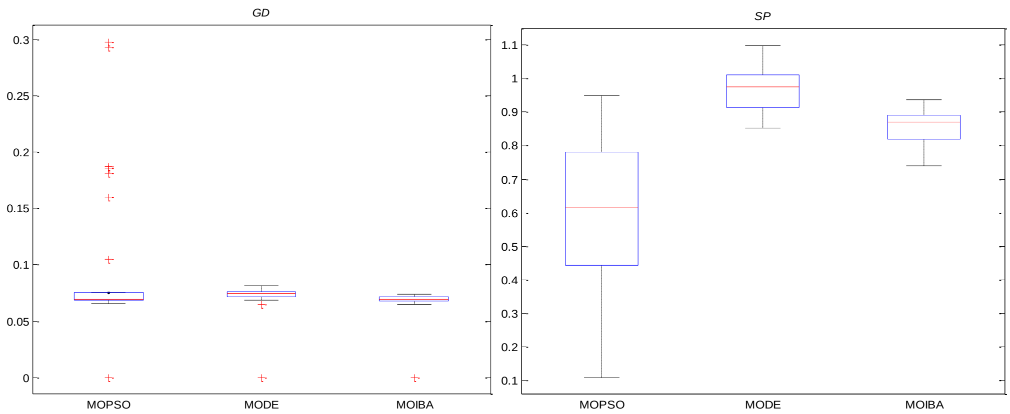

Fig. 14. Boxplots of GD and SP for CASE1

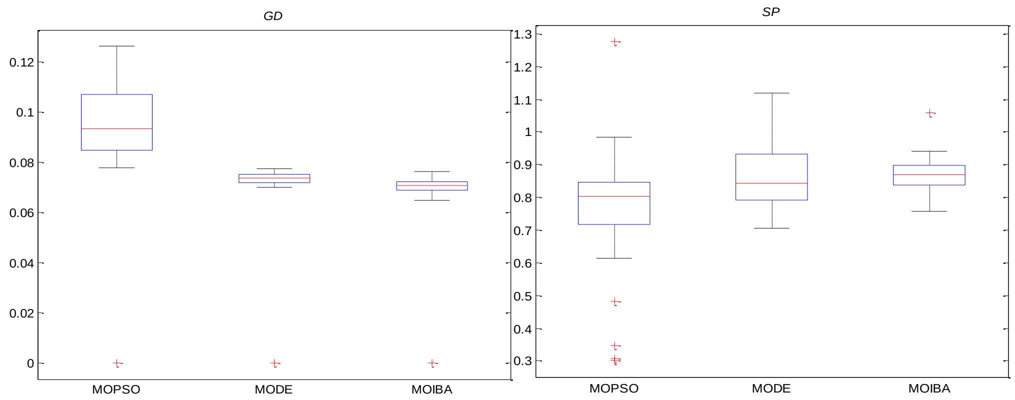

Fig. 15. Boxplots of GD and SP for CASE2

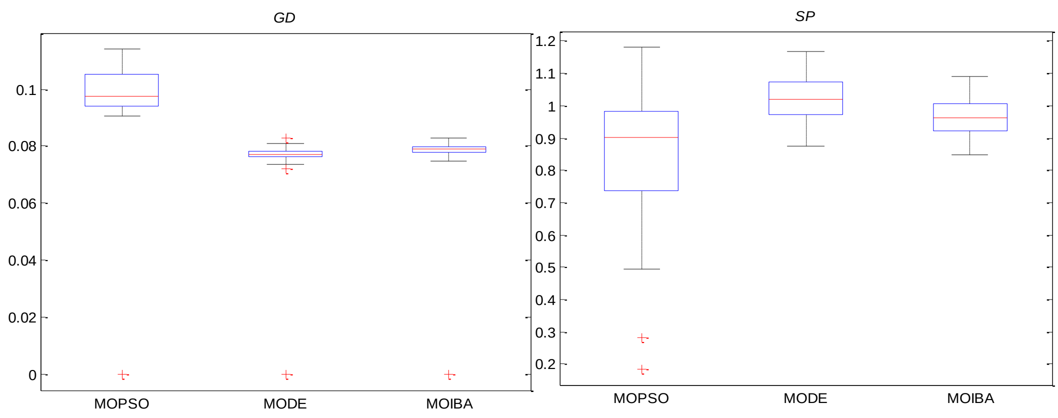

Fig. 16. Boxplots of GD and SP for CASE3

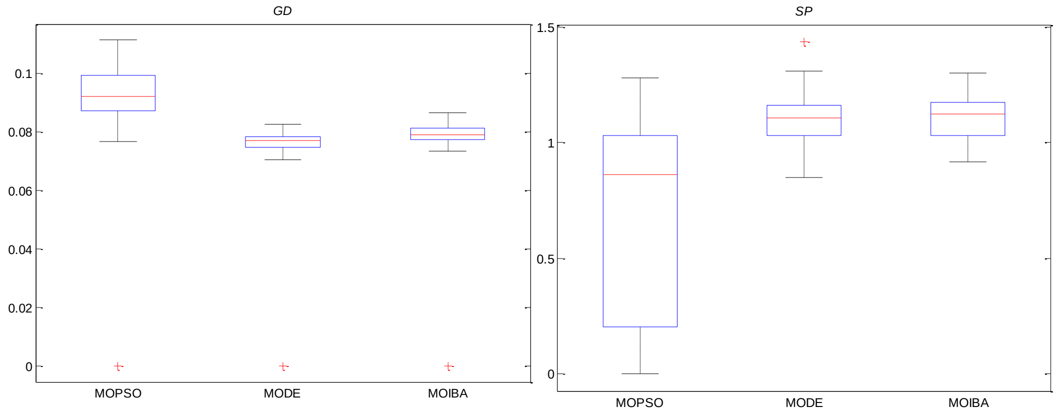

Fig. 17. Boxplots of GD and SP for CASE4

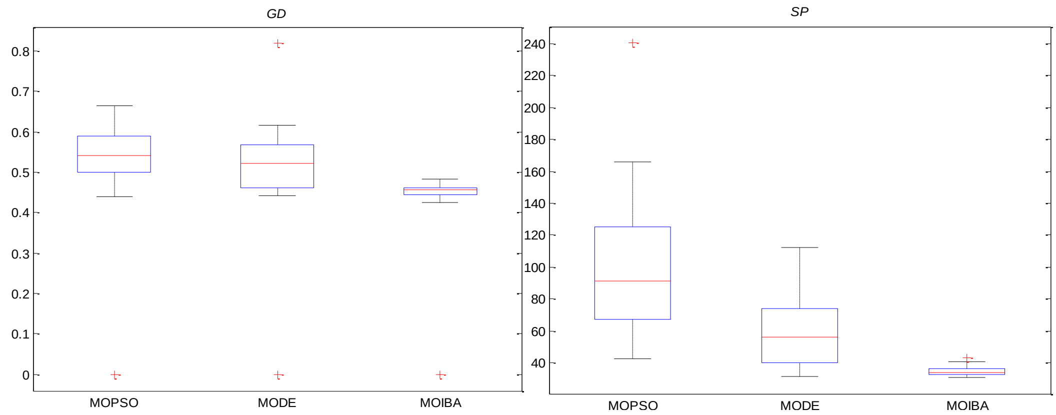

Fig. 18. Boxplots of GD and SP for CASE5

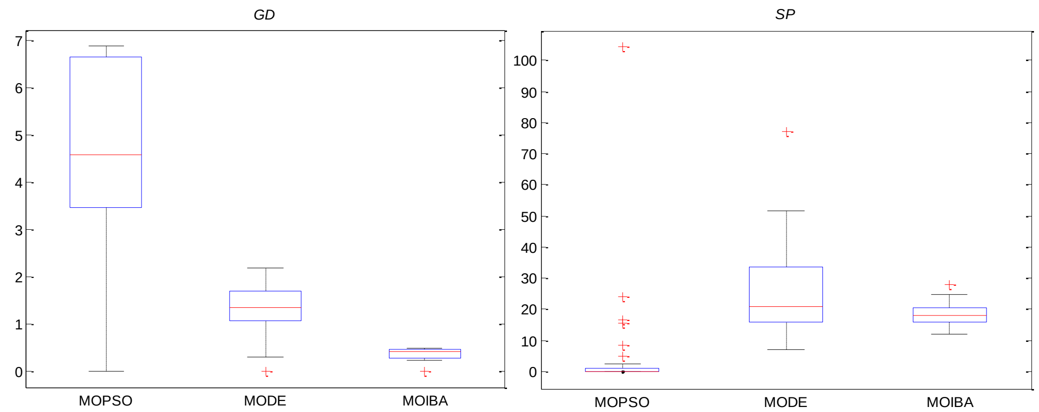

Fig. 19. Boxplots of GD and SP for CASE6

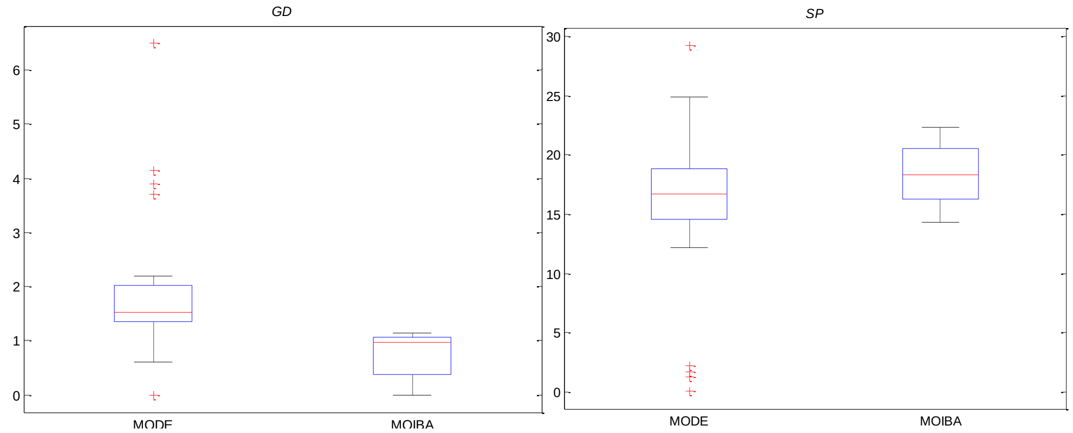

Fig. 20. Boxplots of GD and SP for CASE7

$$SP=\sqrt{\frac{1}{n-1}\sum_{i=1}^{n}\left(d_{mean}-d_i\right)^2} \tag{39}$$

$$d_i=\min_{j=1,2,\cdots,n}\left(\sum_{k=1}^{M}\left|f_k^i-f_k^j\right|\right) \tag{40}$$

$$d_{mean}=\frac{1}{n}\sum_{i}^{n}d_i \tag{41}$$

where d_{mean} represents the mean value of all d_i, which is defined as (41). SP=0 means all optimal solutions at the current PF are spaced equidistantly. That is to say, the closer SP to zero, the better distribution and diversity POS can achieve.

B. GD

To describe the distance between the obtained PF and the real one, criteria of GD is adopted. Exhaustive description and application of GD can be found in [38, 39]. The GD index can be described as (42).

$$GD=\frac{\sqrt{\sum_{i=1}^{n}de_i^2}}{n} \tag{42}$$

where de_i represents Euclidean distance between each of compromise solutions and the nearest one of the real PF. n represents the number of non-dominated solutions. The larger GD value means worse optimization effect of the algorithm. It is considerable to mention that GD=0 means all found solutions are in line with the real PF. Hence, the value of GD criteria is the closer to zero, the PF obtained by MOIBA method is more in conformity with the real one.

C. Boxplot

Boxplot, a statistical tool to describe the dispersion of data set, is utilized in this paper. Boxplot can display the maximum, minimum, median, upper and lower quartile of a dataset [40]. It is worth to mention that boxplot can reveal outliers in a set of data, which is of great significance for avoiding the consequences of neglecting existence of outliers.

In general, the closer boxplot of statistical result is, the better convergence and stability proposed algorithm can achieve. The quantitative data achieved by MOIBA, MOPSO and MODE approaches are collected for statistical study on GD and SP. The boxplots of above seven testing cases are shown in Fig. 14 ~ Fig. 20. The mean and standard deviation of GD and SP for CASE1 ~ CASE7 are shown on TABLE XIII ~ TABLE XVI.

D. Analysis of statistical data

Foremost, metrics of IEEE 30-bus system are analysed. Based on Fig. 14~Fig. 17 , the conclusion that performance of MOIBA with fewer outliers and closer boxplots evidently overmatches MOPSO method can be drawn. Yet, MOIBA does not have a clear competitive advantage in distribution and diversity of POS compared with MODE.

For CASE5 and CASE6, studied in IEEE 57-bus system, MOIBA is capable to get smaller values of GD and SP, which means that the solution set fits the real PF greater and the better diversity can be achieved. In a word, TABLE XV quantitatively demonstrate that MOIBA, contrast to MOPSO and MODE approaches, has greater potential to handle MOOPF problems more steadily. It should be aware from Fig. 19 that there are too many outliers to make MOPSO method lack practicality and feasibility although it obtains the smallest mean value in CASE6.

For CASE7, which is studied on IEEE 118-bus system, MOIBA can achieve less outliers and smaller deviation. That is to say, MOIBA can solve MOOPF problems in power systems with complex structure more effectively.

Comprehensively, compared with commonly used methods MOPSO and MODE, MOIBA can obtain evenly distributed PFs and high-quality BC. Based on indexes of generational distance and spacing, MOIBA is superior to MODE and has certain advantages over MOPSO method, reflected in both better-performance BC and favorable distribution of Pareto non-dominated solutions.

In addition, the specific parameters of three algorithms mentioned in this paper can be found in TABLE XVII.

TABLE XVII
MAIN PARAMETERS OF MOPSO, MODE AND MOIBA

parameters	MOPSO	MODE	MOIBA
population	100	100	100
ERP	100	100	100
maximum iterations	300	300	300
c1	2	--	--
c1	2	--	--
ω(min/max)	0.4/0.9	0.4/0.9	0.4/0.9
F	--	0.6	--
CR	--	0.8	--
f(min/max)	--	--	-2/2
R(min/max)	--	--	0.1/0.5
A(min/max)	--	--	0.5/0.95

VII. Conclusion

A new multi-objective improved bat algorithm named MOIBA, including nonlinear adjustment strategy of inertia weight, global optimal guiding mechanism and monotone random filling model based on extreme, is proposed in this paper. The novel MOIBA algorithm is applied to handle MOOPF problems and seven multi-objective testing cases considering basic fuel cost, fuel cost with value-point loadings, emission and active power loss are carried out on IEEE 30-bus, IEEE 57-bus and IEEE 118-bus systems. To achieve evenly distributed POS and high-quality BC, three strategies known as PMC, ESCD and FAA are taken into account. The GD and SP metrics demonstrate that MOIBA has more powerful competitive advantages than MOPSO and MODE, reflected in not only the preferable BC, but also the favorable distribution and diversity of POS. Therefore, the proposed MOIBA algorithm provides an innovative and reasonable means of dealing with the MOOPF problem.

Acknowledgment

The authors would like to thank the editors and the reviewers for their constructive comments and suggestions.

References

[1] G. Chen, Z. Lu and Z. Zhang, "Improved Krill Herd Algorithm with Novel Constraint Handling Method for Solving Optimal Power Flow Problems," *ENERGIES*, vol. 11, 2018.

[2] D. Prasad, A. Mukherjee, G. Shankar, and V. Mukherjee, "Application of chaotic whale optimisation algorithm for transient stability constrained optimal power flow," *IET SCIENCE MEASUREMENT & TECHNOLOGY*, vol. 11, pp. 1002-1013, 2017.

[3] G. Chen, S. Qiu, Z. Zhang, Z. Sun, and H. Liao, "Optimal Power Flow Using Gbest-Guided Cuckoo Search Algorithm with Feedback Control Strategy and Constraint Domination Rule," *MATHEMATICAL PROBLEMS IN ENGINEERING*, 2017.

[4] A. Attarha and N. Amjady, "Solution of security constrained optimal power flow for large-scale power systems by convex transformation techniques and Taylor series," *IET GENERATION TRANSMISSION & DISTRIBUTION*, vol. 10, pp. 889-896, 2016.

[5] P. P. Biswas, P. N. Suganthan, R. Mallipeddi, and G. A. J. Amaratunga, "Optimal power flow solutions using differential evolution algorithm integrated with effective constraint handling techniques," *Engineering Applications of Artificial Intelligence*, vol. 68, pp. 81-100, 2018-01-01 2018.

[6] Li S, Jiao L, Zhang Y, et al. "A scheme of resource allocation for heterogeneous services in peer-to-peer networks using particle swarm optimization.," *IAENG International Journal of Computer Science*, vol.44, no.4, pp.482-488, 2017..

[7] M. Ghasemi, S. Ghavidel, M. M. Ghanbarian, M. Gharibzadeh, and A. A. Vahed, "Multi-objective optimal power flow considering the cost, emission, voltage deviation and power losses using multi-objective modified imperialist competitive algorithm," *ENERGY*, vol. 78, pp. 276-289, 2014.

[8] B. Mandal and P. K. Roy, "Multi-objective optimal power flow using quasi-oppositional teaching learning based optimization," *APPLIED SOFT COMPUTING*, vol. 21, pp. 590-606, 2014.

[9] E. Dehnavi and H. Abdi, "Optimal pricing in time of use demand response by integrating with dynamic economic dispatch problem," *ENERGY*, vol. 109, pp. 1086-1094, 2016.

[10] X. Yuan, B. Zhang, P. Wang, J. Liang, Y. Yuan, Y. Huang, and X. Lei, "Multi-objective optimal power flow based on improved strength Pareto evolutionary algorithm," *ENERGY*, vol. 122, pp. 70-82, 2017.

[11] T. Ding, C. Li, F. Li, T. Chen, and R. Liu, "A bi-objective DC-optimal power flow model using linear relaxation-based second order cone programming and its Pareto Frontier," *International Journal of Electrical Power & Energy Systems*, vol. 88, pp. 13-20, 2017.

[12] Zheng W, Qiao J, Feng L, et al. "Optimal cooperative virtual multi-input and multi-output network communication by double improved ant colony system and genetic algorithm.," *IAENG International Journal of Computer Science*, vol.45, no.1, pp.89-96, 2018.

[13] Li S, Wang J, " Improved Cuckoo Search Algorithm with Novel Searching Mechanism for Solving Unconstrained Function Optimization Problem," *IAENG International Journal of Computer Science*, vol.44, no.1, pp.8-12, 2017.

[14] S. Sivasubramani and K. S. Swarup, "Multi-objective harmony search algorithm for optimal power flow problem," *International Journal of Electrical Power & Energy Systems*, vol. 33, pp. 745-752, 2011.

[15] T. Niknam, M. R. Narimani, M. Jabbari, and A. R. Malekpour, "A modified shuffle frog leaping algorithm for multi-objective optimal power flow," *ENERGY*, vol. 36, pp. 6420-6432, 2011.

[16] M. R. Narimani, R. Azizipanah-Abarghooee, B. Zoghdar-Moghadam-Shahrekohne, and K. Gholami, "A novel approach to multi-objective optimal power flow by a new hybrid optimization algorithm considering generator constraints and multi-fuel type," *ENERGY*, vol. 49, pp. 119-136, 2013.

[17] V. S. Kumar, M. R. Thansekhar, R. Saravanan, and S. M. J. Amali, "Solving Multi-objective Vehicle Routing Problem with Time Windows by FAGA," in *Procedia Engineering*. vol. 97, M. A. Xavior and P. Yarlagadda, Eds., 2014, pp. 2176-2185.

[18] B. Mahdad and K. Srairi, "Security constrained optimal power flow solution using new adaptive partitioning flower pollination algorithm," *APPLIED SOFT COMPUTING*, vol. 46, pp. 501-522, 2016.

[19] J. Zhang, Q. Tang, P. Li, D. Deng, and Y. Chen, "A modified MOEA/D approach to the solution of multi-objective optimal power flow problem," *APPLIED SOFT COMPUTING*, vol. 47, pp. 494-514, 2016.

[20] B. Mahdad and K. Srairi, "Security constrained optimal power flow solution using new adaptive partitioning flower pollination algorithm," *APPLIED SOFT COMPUTING*, vol. 46, pp. 501-522, 2016.

[21] S. S. Reddy and C. S. Rathnam, "Optimal Power Flow using Glowworm Swarm Optimization," *International Journal of Electrical Power & Energy Systems*, vol. 80, pp. 128-139, 2016.

[22] K. Deb and H. Jain, "An Evolutionary Many-Objective Optimization Algorithm Using Reference-Point-Based Nondominated Sorting Approach, Part I: Solving Problems With Box Constraints," *IEEE TRANSACTIONS ON EVOLUTIONARY COMPUTATION*, vol. 18, pp. 577-601, 2014.

[23] O. T. Altinoz, K. Deb and A. E. Yilmaz, "Evaluation of the migrated solutions for distributing reference point-based multi-objective optimization algorithms," *INFORMATION SCIENCES*, vol. 467, pp. 750-765, 2018.

[24] K. Deb, A. Pratap, S. Agarwal, and T. Meyarivan, "A fast and elitist multiobjective genetic algorithm: NSGA-II," *IEEE Trans. Evol. Comput*, pp. 182-197, 2002.

[25] G. Chen, X. Yi, Z. Zhang, and H. Wang, "Applications of multi-objective dimension-based firefly algorithm to optimize the power losses, emission, and cost in power systems," *APPLIED SOFT COMPUTING*, vol. 68, pp. 322-342, 2018.

[26] T. K. Tharakeshwar, K. N. Seetharamu and B. D. Prasad, "Multi-objective optimization using bat algorithm for shell and tube heat exchangers," *Applied Thermal Engineering*, vol. 110, 2017.

[27] B. R. Adarsh, T. Raghunathan, T. Jayabarathi, and X. Yang, "Economic dispatch using chaotic bat algorithm," *ENERGY*, vol. 96, pp. 666-675, 2016.

[28] Y. Yuan, X. Wu, P. Wang, and X. Yuan, "Application of improved bat algorithm in optimal power flow problem," *APPLIED INTELLIGENCE*, vol. 48, pp. 2304-2314, 2018.

[29] S. Dhar and M. K. Kundu, "A novel method for image thresholding using interval type-2 fuzzy set and Bat algorithm," *APPLIED SOFT COMPUTING*, vol. 63, pp. 154-166, 2018-01-01 2018.

[30] D. Igrec, A. Chowdhury, B. Stumberger, and A. Sarjas, "Robust tracking system design for a synchronous reluctance motor - SynRM based on a new modified bat optimization algorithm," *APPLIED SOFT COMPUTING*, vol. 69, pp. 568-584, 2018-01-01 2018.

[31] A. A. Mohamed, Y. S. Mohamed, A. A. M. El-Gaafary, and A. M. Hemeida, "Optimal power flow using moth swarm algorithm," *ELECTRIC POWER SYSTEMS RESEARCH*, vol. 142, pp. 190-206, 2017.

[32] M. Ghasemi, S. Ghavidel, M. M. Ghanbarian, and M. Gitizadeh, "Multi-objective optimal electric power planning in the power system using Gaussian bare-bones imperialist competitive algorithm," *INFORMATION SCIENCES*, vol. 294, pp. 286-304, 2015.

[33] A. E. Chaib, H. R. E. H. Bouchekara, R. Mehasni, and M. A. Abido, "Optimal power flow with emission and non-smooth cost functions using backtracking search optimization algorithm," *International Journal of Electrical Power & Energy Systems,* vol. 81, pp. 64-77, 2016.
[34] M. Ghasemi, S. Ghavidel, J. Aghaei, M. Gitizadeh, and H. Falah, "Application of chaos-based chaotic invasive weed optimization techniques for environmental OPF problems in the power system," *CHAOS SOLITONS & FRACTALS,* vol. 69, pp. 271-284, 2014.
[35] N. Daryani, M. T. Hagh and S. Teimourzadeh, "Adaptive group search optimization algorithm for multi-objective optimal power flow problem," *APPLIED SOFT COMPUTING,* vol. 38, pp. 1012-1024, 2016.
[36] H. Pulluri, R. Naresh and V. Sharma, "An enhanced self-adaptive differential evolution based solution methodology for multiobjective optimal power flow," *APPLIED SOFT COMPUTING,* vol. 54, pp. 229-245, 2017.
[37] S. Sivasubramani and K. S. Swarup, "Multi-objective harmony search algorithm for optimal power flow problem," *International Journal of Electrical Power & Energy Systems,* vol. 33, pp. 745-752, 2011.
[38] H. Ishibuchi, H. Masuda, Y. Tanigaki, and Y. Nojima, "Modified Distance Calculation in Generational Distance and Inverted Generational Distance," in *Lecture Notes in Computer Science*. vol. 9019, A. GasparCunha, C. H. Antunes and C. C. Coello, Eds., 2015, pp. 110-125.
[39] M. Li, S. Yang and X. Liu, "Shift-Based Density Estimation for Pareto-Based Algorithms in Many-Objective Optimization," *IEEE TRANSACTIONS ON EVOLUTIONARY COMPUTATION,* vol. 18, pp. 348-365, 2014.
[40] D. F. Williamson, R. A. Parker and J. S. Kendrick, "The box plot: a simple visual method to interpret data.," *Annals of internal medicine,* vol. 110, pp. 916-21, 1989.